Journal of Statistical Physics, Vol. 122, No. 5, March 2006 (© 2006)
DOI: 10.1007/s10955-005-9004-8

Front Propagation Dynamics with Exponentially-Distributed Hopping

Elisheva Cohen[1] and David A. Kessler[1]

Received 4 August 2005; accepted 15 November 2005
Published Online: March 10, 2006

We study reaction-diffusion systems where diffusion is by jumps whose sizes are distributed exponentially. We first study the Fisher-like problem of propagation of a front into an unstable state, as typified by the A+B $\rightarrow$ 2A reaction. We find that the effect of fluctuations is especially pronounced at small hopping rates. Fluctuations are treated heuristically via a density cutoff in the reaction rate. We then consider the case of propagating up a reaction rate gradient. The effect of fluctuations here is pronounced, with the front velocity increasing without limit with increasing bulk particle density. The rate of increase is faster than in the case of a reaction-gradient with nearest-neighbor hopping. We derive analytic expressions for the front velocity dependence on bulk particle density. Computer simulations are performed to confirm the analytical results.

KEY WORDS: Front propagation, reaction-diffusion.

Many physical, chemical, and biological systems exhibit fronts which propagate through space. Familiar examples range from chemical reaction dynamics such as flames[1], phase transitions such as solidification[2], the spatial spread of infections[3], and even the fixation of a beneficial allele in a population[4]. It is thus of great interest to understand the universality classes of fronts which govern what will happen when systems such as these are prepared in a spatially heterogeneous manner. These classes determine the selection of propagation speed, the sensitivity to particle-number fluctuations, and the stability of the front with respect to deviations from planarity.

The simplest kind of such a front is that wherein a stable phase replaces a metastable one[2]. Here the mean-field front velocity is determined via the requirement that there exists a heteroclinic trajectory of the moving-frame steady-state problem (wherein the solution depends only on $x - vt$) connecting the metastable

[1] Department of Physics, Bar-Ilan University, Ramat-Gan, IL52900 Israel.

phase at $+\infty$ with the stable one at $-\infty$. This type of front is robust with respect to fluctuations, with power-law corrections in $1/N$ (where N is the number of particles per site in the final state) to the mean-field limit [5]. A second class is exemplified by the simple infection model $A + B \to 2A$ on a 1d lattice (with spacing a) with on-site reaction with equal A and B hopping rates[3]; this process leads in the mean-field limit to a spatially discrete version of the Fisher equation[4]

$$\dot{\phi}(x) = r\phi(x)(1-\phi(x)) + \frac{D}{a^2}(\phi(x+a) - 2\phi(x) + \phi(x-a)). \qquad (1)$$

Here propagation is into the linearly unstable $\phi = 0$ state, where ϕ is the number of A particles at a site. Recent work[5–8] has shown that the front behavior in the stochastic model does approach that of the Fisher equation, where the velocity is selected by the (linear) marginal stability criterion[9] to be $2\sqrt{rD}$, albeit with an anomalously long transient $O(1/t)$ and anomalously large fluctuation corrections $O(1/\ln^2 N)$. The key technical tool which has allowed progress in treating the stochastic model is the observation that introducing[6,10,11] a cutoff in the reaction term when the density of particles falls below some threshold reproduces the major effects caused by the discrete nature of the reacting particles[12]. There are also some findings in regard to both front stability in the case of unequal D[13], and also the scaling properties of front fluctuations[14]. Finally, there are also fronts which have properties intermediate to the previous two classes.

In a recent work[15,16], we introduced a new class of fronts corresponding to propagation into an unstable state up a reaction-rate gradient[17,18]. This type of gradient is present, for example, in systems with an inherent spatial inhomogeneity, and also in models of Darwinian evolution[19–22], (where the birth rate, which is parallel to our reaction rate, is proportional to fitness x). We found that the sensitivity to fluctuations in the presence of such a positive reaction-rate gradient is greatly enhanced. In particular, the front velocity diverges with increasing bulk particle density. As a corollary, the standard reaction-diffusion equation treatment is not useful, as it gives rise to finite-time singularities in the velocity. Also, the velocity is strongly sensitive to details of diffusion, with the increase of the velocity with density being qualitatively stronger for a lattice system than in the continuum.

Given this sensitivity to the precise implementation of diffusion, in this work we turn to the study the effect of implementing diffusion via infinite-range hopping, where the size of the jumps is distributed exponentially. Such a model has been considered, for example, in the description of the airborne dispersion of seeds, leading to the spread of a particular colony of plants[23]. It is also relevant in the evolution context, where the change in fitness due to mutations is commonly assumed to be exponentially distributed[24]. We will see that even in the absence of a gradient, this form of diffusion increases dramatically the effect of fluctuations, at least for small hopping rates. In particular, the naive reaction-diffusion formalism predicts a finite velocity in the limit of zero hopping rate, which is

clearly unphysical, given the on-site nature of the reaction. Introducing a reaction-rate gradient again changes the functional dependence of the velocity on density from that of the nearest-neighbor hopping studied previously.

The plan of the paper is as follows. In Sec. 1, we discuss the gradient-free model, and derive the velocity in the limit of infinite density. We show that for fixed hopping rate, the finite density correction formula derived by Brunet and Derrida for the Fisher equation is applicable. However, this formula breaks down in the small hopping rate limit. We derive an analytical expression for the velocity in this limit. In Sec. 2, we discuss a similar model of Snyder[23] designed to model the spread of colonies, showing that the same physics applies upon the appropriate mapping of parameters. In Sec. 3, we introduce our reaction-rate gradient model, and after briefly reviewing what is known for continuum diffusion and nearest-neighbor hopping, we calculate an analytical approximation to the velocity for large density. Finally, in Sec. 4, we summarize our results and draw some conclusions. Technical details on the numerical and simulational procedures are relegated to an appendix.

1. EXPONENTIAL HOPPING FISHER EQUATION

As a prototypical system, we consider a long-range hopping version of the $A + B \to 2A$ infection model previously considered for the case of nearest-neighbor hopping[3,5,6]. The model is defined on a 1-D lattice with no restriction on multiple occupancy of sites. The initial state is taken to be a constant number N of B particles on every site, with a single A introduced at the left-most site. An A and B particle residing on the same site have some probability per unit time r/N of interacting and transforming the B to an A. We implement long-range hopping by taking the hopping probability per unit time to have an unbounded range, decreasing exponentially with distance [25]. (See the appendix for details on simulating this model.) The naive reaction-diffusion description of this stochastic particle model is a type of Fisher equation [4], with a modified diffusion term: In the continuum limit, this equation reads:

$$\dot{\phi}(x) = \frac{D\beta^3}{2} \int_0^\infty ds e^{-\beta s} \left(\phi(x+s) + \phi(x-s)\right) - D\beta^2 \phi(x) + r\phi(x)\left(1 - \phi(x)\right), \tag{2}$$

where $\phi(x)$ is the density of A's at x, relative to the initial (constant) density of B's. The steady-state equation is:

$$\frac{D\beta^3}{2} \int_0^\infty ds e^{-\beta s} \left(\phi(x+s) + \phi(x-s)\right) - D\beta^2 \phi(x) + v\phi'(x) + r\phi(x)\left(1 - \phi(x)\right)) = 0. \tag{3}$$

It is useful to convert this equation into a differential equation using the fact that

$$O_{\pm}\int_0^{\infty} ds e^{-\beta s}\phi(x \pm s) \equiv \left(\beta \mp \frac{d}{dx}\right)\int_0^{\infty} ds e^{-\beta s}\phi(x \pm s) = \phi(x). \quad (4)$$

Then, acting upon Eq. (3) by O_+O_- yields

$$D\beta^2\phi'' + \left(\beta^2 - \frac{d^2}{dx^2}\right)(v\phi' + r\phi(1-\phi)) = 0 \quad (5)$$

Our first task, then, is to study this equation, comparing it to the standard Fisher equation, as a preliminary to discussing its defects as a description of our stochastic $A + B \to 2A$ model. As with the standard Fisher equation, this equation has solutions for all velocities, and positive definite solutions for all velocities greater than some critical velocity, the so-called marginally stable velocity, v_F, which is the asymptotic velocity of propagation of all fronts with initial compact support. This can be found from the dispersion relation for the leading edge where $\phi \sim e^{-kx}$:

$$D\beta^2k^2 + (\beta^2 - k^2)(-vk + r) = 0 \quad (6)$$

The marginally stable velocity, v_F, is then given by the requirement that Eq. (6) has a degenerate solution, leading to the discriminant condition

$$0 = \frac{d}{dk}\left[D\beta^2k^2 + (\beta^2 - k^2)(-vk + r)\right] = 2D\beta^2k - \beta^2v + 3vk^2 - 2rk. \quad (7)$$

Solving simultaneously Eqs. (6) and (7) yields, introducing $t \equiv \sqrt{D^2\beta^4 + 8D\beta^2r}$

$$v_F = \frac{\sqrt{2}(5D\beta^2 + 4r + 3t)}{8\beta}\sqrt{\frac{D\beta^2 + 2r - t}{r - D\beta^2}} \quad (8)$$

This has the scaling form $v_F = 2\sqrt{rD}f(\beta^2D/r)$ where the function $f(x) \to 1$ for $x \to \infty$ and $f(x) \sim 1/(2\sqrt{x})$ as $x \to 0$. Thus, for large β, we recover the usual Fisher answer, which is reasonable since in this limit the hopping is effectively short-range. What is remarkable is that the velocity has the finite limit r/β as $D \to 0$, so that we have velocity without diffusion!

1.1. Calculation of the Velocity for a Small Cutoff

This anomaly is yet another example of how the reaction diffusion equation, Eq. (2), provides incorrect information about the original stochastic model. A more accurate picture is achieved by studying a cutoff version of the equation, wherein the reaction is turned off wherever $\phi(x)$ is less than some threshold ϵ, of order $1/N$[5,6,10,11,19]. This captures an essential feature of the original model, namely that the reaction zone always has compact support. Brunet and Derrida[6]

have provided a general formula for the correction induced in the velocity due to the cutoff (for small cutoffs) for Fisher-like equations. This formula reads

$$v_\epsilon = v_F - \frac{v''(k_F)\pi^2 k_F^2}{2(\ln \epsilon)^2}. \tag{9}$$

where k_F is the degenerate solution of the dispersion relation, Eq. (6). Although derived for second order equations, whereas our equation is of third order, nevertheless, as we shall see, it correctly gives the leading order correction for the velocity in our case as well.

1.1.1. Jump Conditions at the Cutoff Point

The first task, as for the standard Fisher equation, is to solve the equation for the region beyond the cutoff, where $\phi(x) < \epsilon$. This will give a set of boundary conditions at the cutoff point, x_c. Due to the third-order nature of our equations, and that the derivatives act on the now discontinuous reaction term, these conditions are fairly messly. While the solution is continuous at the cutoff point, there is no continuity of the first and second derivatives at this point.

To derive the correct jump conditions, we start from the integral equation, Eq. (3). For the rightmost region, $x > x_c$, the solution is $\phi_x = \epsilon e^{-k_r(x-x_c)}$, where k_r satisfies the $r = 0$ dispersion relation

$$D\beta^2 k_r^2 - \left(\beta^2 - k_r^2\right) v k_r = 0 \tag{10}$$

or,

$$k_r = \frac{-D\beta^2 + \sqrt{D^2\beta^4 + 4\beta^2 v^2}}{2v} \tag{11}$$

Thus,

$$\int_0^\infty ds e^{-\beta s}\phi(x_c + s) = \frac{\epsilon}{\beta + k_r} \tag{12}$$

Evaluating the integral equation, Eq. (3), as $x \to x_c^+$ gives

$$\frac{D\beta^3}{2}\left[\frac{\epsilon}{\beta + k_r} + \int_0^\infty ds e^{-\beta s}\phi(x_c - s)\right] - D\beta^2\epsilon - v k_r \epsilon = 0 \tag{13}$$

This, together with Eq. (10), yields

$$\int_0^\infty ds e^{-\beta s}\phi(x_c - s) = \frac{\epsilon}{\beta - k_r} \tag{14}$$

Now, let us analyze Eq. (3) for $x \to x_c^-$. We get

$$\phi'(x_c^-) = -\frac{r\epsilon(1-\epsilon)}{v} - k_r\epsilon \tag{15}$$

We break up Eq. (3) as follows,

$$0 = \frac{D\beta^3}{2}\left[\int_0^{x_c-x} ds e^{-\beta s}\phi(x+s) + \int_{x_c-x}^{\infty} ds e^{-\beta s}\phi(x+s) + \int_0^{\infty} ds e^{-\beta s}\phi(x-s)\right] - D\beta^2\phi + v\phi' + r\phi(1-\phi)$$

$$= \frac{D\beta^3}{2}\left[e^{-\beta(x_c-x)}\frac{\epsilon}{\beta+k_r} + e^{\beta(x_c-x)}\frac{\epsilon}{\beta-k_r} - 2\int_0^{x_c-x} ds \sinh(\beta s)\phi(x+s)\right] - D\beta^2\phi + v\phi' + r\phi(1-\phi) \tag{16}$$

and upon taking a derivative and evaluating at x_c^- we get

$$\frac{D\beta^3}{2}\left[\beta\frac{\epsilon}{\beta+k_r} - \beta\frac{\epsilon}{\beta-k_r}\right] - D\beta^2\phi'(x_c^-) + v\phi''(x_c^-) + r\phi'(x_c^-)(1-2\phi(x_c^-)) = 0 \tag{17}$$

or

$$\phi''(x_c^-) = \epsilon\frac{-\beta^2 vr + v^2k_r^3 + 2vrk_r^2 + r^2k_r}{k_r v^2} + \epsilon^2\frac{\beta^2 vr - 3vrk_r^2 - 3r^2k_r}{k_r v^2} + \epsilon^3\frac{2r^2}{v^2}. \tag{18}$$

1.1.2. The Modified BD Treatment

As in the original BD treatment, we divide the range of $x < x_c$ into two regions. In the first region, $\phi(x)$ is not small compared to 1, but the effect of the cutoff is negligible. In the second region $\epsilon < \phi(x) << 1$. We fix the translation invariance by requiring $\phi(0) = 1/2$. Then as $\epsilon \to 0$, $x_c \to \infty$. In the first region, we can take the velocity to be v_F, so that there is a degenerate solution of the dispersion relation. Then, for large x, the dominant solution is

$$\phi(x) \sim Axe^{-k_F x} \tag{19}$$

In the second region, since the velocity is close to v_F, $v_\epsilon = v_F - \Delta$, $\Delta \ll 1$, the general solution is:

$$\phi(x) \sim Be^{-k_F x}\sin(k_i x + C) + Fe^{-k_2 x}. \tag{20}$$

where $k_2 < 0$ is the third (nondegenerate) root of the dispersion relation and $k_i \sim \sqrt{\Delta}$ and we can ignore the $0(\Delta)$ shift in the real part of k. Matching between the first and the second region requires that $B = A/k_i$, $C = 0$ and $Fe^{-(k_2-k_F)x_c} \ll 1$. Now, in general, we have to enforce three jump conditions, (whose left hand sides

are Δ-independent to leading order), with the two free parameters B and F, which is impossible. The only way to make things work is to have $\sin(k_i x_c)$ be of the same order as $k_i \cos(k_i x_c)$, in other words $k_i x_c \approx \pi - O(\Delta^{1/2})$, which is exactly the same condition as in the original BD treatment, where there was one free parameter and two jump conditions. Since

$$k_i = \sqrt{\frac{2\Delta}{v''(k_F)}} \tag{21}$$

we immediately recover the BD result quoted above, Eq. (9).

Examining the BD result, we see that in the limit of $D\beta^2/r \gg 1$, $k_F \sim \sqrt{r/D}$ and $v''(k_F) \sim 2\sqrt{D^3/r}$, so that

$$v_\epsilon \sim v_F - \frac{\pi^2 \sqrt{rD}}{\ln^2 \epsilon} \tag{22}$$

which is of course the Fisher result. On the other hand, when $D\beta^2/r \ll 1$, $k_F \sim \beta - \beta^2\sqrt{D/2r}$ and $v''(k_F) \sim (2r)^{3/2}/\beta^4/\sqrt{D}$, and so

$$v_\epsilon \sim v_F - \frac{\pi^2 (2r)^{3/2}}{2\beta^2 \sqrt{D} \ln^2 \epsilon} \tag{23}$$

Thus the BD correction diverges as $D \to 0$. Thus, while for sufficiently small ϵ, the BD correction is correct, for a given ϵ, the BD correction fails for small enough D. We show in Figs. 1 and 2 a plot of v_F and the BD velocity for $\epsilon = 10^{-5}$, compared to the results of an exact numerical calculation. In Fig. 2 it can be seen as predicted that the BD treatment does not apply for small D. A calculation in this limit is presented in the next subsection.

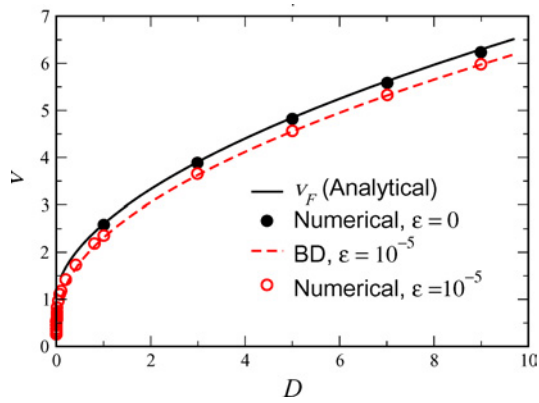

Fig. 1. v vs. large D for exponential Fisher model. Analytical formula for v_0 (8), and analytical formula for v_ϵ (9), compared to numerical results. $\epsilon = 10^{-5}$, $\beta = 1$. (color online).

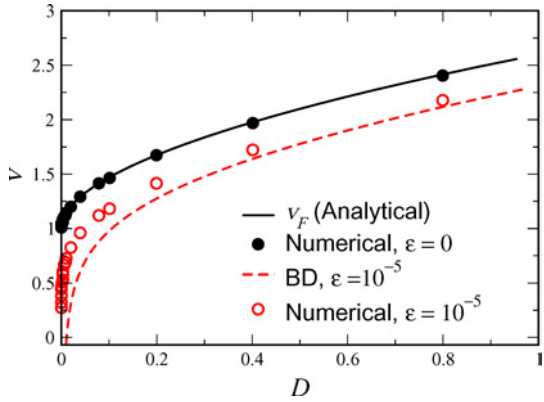

Fig. 2. v vs. small D for exponential Fisher model. Analytical formula for v_0 (8), and analytical formula for v_ϵ (9), compared to numerical results. $\epsilon = 10^{-5}$, $\beta = 1$ (color online).

1.2. Small D, Small ϵ Limit

Clearly, in the presence of a cutoff, the velocity should vanish as $D \to 0$. Let us solve the model in this limit. First, let us examine what happens when $D = 0$. Then, for small ϵ we can linearize around the $\epsilon = 0$ solution $\phi_0 = \frac{1}{1+e^{rx/v}}$, writing $\phi = \phi_0 + \delta$. The equation for δ reads

$$\left(\beta^2 - \frac{d^2}{dx^2}\right)\left(v\delta' + r\delta(1 - 2\phi_0)\right) = 0 \tag{24}$$

The general solution with $\delta(0) = 0$, so that the center of the front does not move, is given by

$$\delta = \frac{1}{v\cosh^2\left(\frac{rx}{2v}\right)} \int_0^x \cosh^2\left(\frac{rx}{2v}\right)\left(Ae^{-\beta x} + Be^{\beta x}\right) \tag{25}$$

What is important is the large-x asymptotics of δ:

$$\delta \sim \frac{A}{r - \beta v}e^{-\beta x} + \frac{B}{r + \beta v}e^{\beta x} \tag{26}$$

We can now use the jump conditions, with $k_r = \beta$ since $D = 0$, to fix x_c, A and B. We get, to leading order in ϵ,

$$\begin{aligned} e^{-rx_c/v} &= \epsilon\frac{r}{r - \beta v} \\ Ae^{-\beta x_c} &= -\epsilon v\beta \\ B &= 0 \end{aligned} \tag{27}$$

The interesting question is now the behavior at $x \to -\infty$. The leading asymptotics is

$$\delta \sim -\frac{A}{r+\beta v} e^{-\beta x} \tag{28}$$

which diverges and so violates the boundary conditions. Thus, there is no solution without D. To leading order in D, we get an inhomogeneous term, $D\beta^2\phi_0''$, on the left-hand-side of Eq. (24). The inhomogeneous solution, δ_D, then satisfies the equation

$$v\delta_D' + r\tanh\left(\frac{rx}{2v}\right)\delta_D = \int_{-\infty}^{\infty} dy G(x-y)\left(\frac{-D\beta^2 r^2}{4v^2}\right)\frac{\sinh\left(\frac{ry}{2v}\right)}{\cosh^3\left(\frac{ry}{2v}\right)} \tag{29}$$

where G is the Green's function for the operator $\beta^2 - \frac{d^2}{dx^2}$,

$$G(x-y) = \frac{1}{2\beta} e^{-\beta|x-y|} \tag{30}$$

so that

$$\delta_D = \frac{1}{v\cosh^2\left(\frac{rx}{2v}\right)}\int_0^x dx' \cosh^2\left(\frac{rx'}{2v}\right)\int_{-\infty}^{\infty} dy G(x'-y)\left(\frac{-D\beta^2 r^2}{4v^2}\right)\frac{\sinh\left(\frac{ry}{2v}\right)}{\cosh^3\left(\frac{ry}{2v}\right)} \tag{31}$$

We need the asymptotic behavior of δ_D for large x. For $r/v \gg \beta$, the integral is dominated by the region of x' large, $y \approx 0$. Thus,

$$\begin{aligned}
\delta_D &\sim \frac{4e^{-rx/v}}{v}\int_{-\infty}^{x} dx' \frac{e^{rx'/v}}{4}\int_{-\infty}^{\infty} dy \frac{e^{-\beta x'}}{2\beta}\left(1+\beta y+\frac{\beta^2 y^2}{2}+\cdots\right)\left(\frac{-D\beta^2 r^2}{4v^2}\right)\frac{\sinh\left(\frac{ry}{2v}\right)}{\cosh^3\left(\frac{ry}{2v}\right)} \\
&= -\frac{D\beta r^2}{8v^3} e^{-rx/v}\int_{-\infty}^{x} dx' e^{rx'/v} e^{-\beta x'}\left(\beta\left(\frac{2v}{r}\right)^2 + \frac{\beta^3}{8}\left(\frac{2v}{r}\right)^4 \frac{\pi^2}{4}+\cdots\right) \\
&= -\frac{D\beta^2}{2v}\frac{1}{\frac{r}{v}-\beta} e^{-\beta x}\left(1+\frac{\beta^2 v^2\pi^2}{8r^2}+\cdots\right)
\end{aligned} \tag{32}$$

We now have to again solve the jump conditions with this new contribution. The coefficient A above is now modified and includes a term which, up to linear order in $\beta v/r$, reads

$$A_D = \frac{\beta^2 D}{2}\left(1+\frac{\beta v}{r}\right) \tag{33}$$

The condition for a solution is that this cancels the A we found above, so that

$$\frac{\beta^2 D}{2}\left(1+\frac{\beta v}{r}\right) = \epsilon v\beta e^{\beta x_c} \tag{34}$$

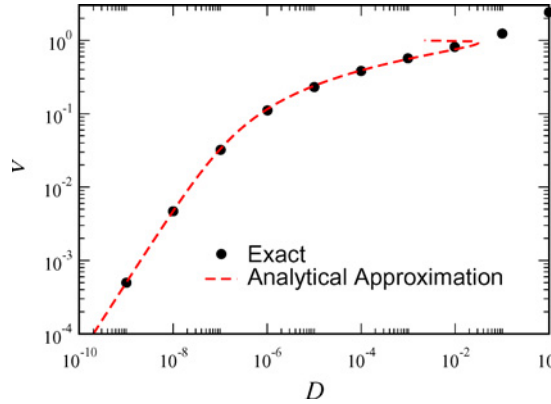

Fig. 3. Comparison of our analytic approximation, Eq. (35) and an exact numerical solution of Eq. (5). Parameters are $\epsilon = 10^{-6}$, $\beta = r = 1$. (color online).

or

$$D = \frac{2\epsilon v}{\beta\left(1+\frac{\beta v}{r}\right)} e^{-\beta v/r \ln(\epsilon r/(r-\beta v))} = \frac{2vr}{\beta(r+\beta v)} \epsilon^{1-\beta v/r} \left(\frac{r}{r-\beta v}\right)^{-\beta v/r} \quad (35)$$

Thus, for very small D, the velocity is equal to $D\beta/(2\epsilon)$, which is reminiscent of the behavior of evolution models for very small mutation rates[20]. The comparison between our analytic approximation and an exact numerical solution is shown in Fig. (3). We see that the approximation does very well until v is close to r/β, when our approximation has D decreasing to 0, and so clearly breaks down.

2. THE SNYDER DISCRETE-TIME MODEL

Recently, Snyder[23] introduced a model of colony spreading which, in one variant, involved an exponentially-distributed hopping similar to the model defined above. The essential difference between her model and ours is that hers was a discrete-time model. In each time step, all the offspring performed a hop and the parental generation was removed. The number of offspring at a given site was given by a local logistic growth law, similar to that incorporated in the Fisher model. Snyder performed numerical simulations and measured the velocity of propagation, both for the stochastic model, and for the corresponding (uncutoff) reaction-diffusion system, and found a difference between these two velocities. Due to its close correspondence to the present model under investigation, it is useful to derive analytically the uncutoff velocity and the BD approximation to the cutoff velocity, so as to make clear the mapping between the Snyder model and ours.

As always, to derive the uncutoff "Fisher" (marginally-stable) velocity, it is enough to consider the linearized version of the Snyder model, which reads

$$\phi^{t+1}(x) = \frac{r_S \beta}{2} \int_{-\infty}^{\infty} \phi^t(y) e^{-\beta|y-x|} dy \tag{36}$$

where r_S is the average number of offspring per individual and $\phi^t(y)$ is the number of individuals at site y at (integer) time t. We assume that the dependence of ϕ on t and y is

$$\phi^t(y) = \phi(y - vt), \tag{37}$$

and

$$\phi^t(y) = e^{-\alpha(y-tv)}. \tag{38}$$

putting (38) in (36) yields:

$$e^{\alpha v} = \frac{r_S \beta^2}{\beta^2 - \alpha^2}\ . \tag{39}$$

Taking the derivative by α of (39) (according to the marginal stability criterion), and dividing it by (39) yields:

$$v_F = \frac{2\alpha_F}{\beta^2 - \alpha_F^2}\ . \tag{40}$$

We can eliminate α_F to obtain a direct relationship between r and v_F as follows:

$$\alpha_F = \frac{-1 + \sqrt{v_F^2 \beta^2 + 1}}{v_F}. \tag{41}$$

so

$$r_S = \frac{2\left(\sqrt{1 + v_F^2 \beta^2} - 1\right) e^{\sqrt{v_F^2 \beta^2 + 1} - 1}}{v_F^2 \beta^2}, \tag{42}$$

It is reassuring that this formula reproduces the velocity measured by Snyder for the one set of parameters presented in her paper. For r_S near 1, $v \sim 2\sqrt{(r_S - 1)/2}/\beta$, while for large r_S, $v \sim \ln(r_S)/\beta$. Of course, on dimensional grounds this is reasonable, since v is a velocity per round, which has units of length, and r_S is dimensionless. We see that r_S near 1 corresponds to the Fisher limit, equivalent to the large $D\beta^2/r$ limit of our model, since the growth rate of the population is $r_S - 1$, so that small $r_S - 1$ corresponds to a large value of our dimensionless control parameter. The two models agree also at large r_S, since in one round of time extent Δt, the population increases by a factor $e^{r\Delta t} - 1$, which is just r_S, so that $r = \ln(r_S)/\Delta t$. Plugging this into the results for our model for

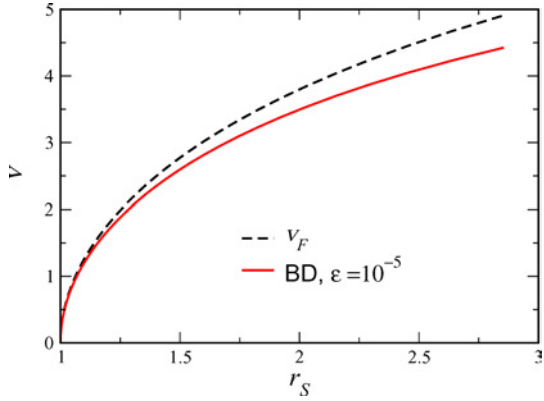

Fig. 4. Snyder model: v_F vs. r_S according to (40) and the BD correction v_ϵ vs r_S. $\beta = 0.5$ (color online).

large r, the velocity is r/β, which is $\ln(r_S)/(\beta\Delta t)$. The distance travelled in one round is the $\ln(r_S)/\beta$, exactly as in the Snyder model. Equivalently, for small D in our model, the time for one round in the Snyder model is proportional to $1/D$, since in the Snyder model, everyone hops in every round, so the weaker diffusion is, the longer a Snyder round must be to allow time for everyone to hop. Thus, for a given r, r_S is very large, and so by the above argument the distance travelled in one round is large, proportional to $1/D$. But, since the duration of the round also scales as $1/D$, the velocity per unit time in our model remains finite, as we have seen.

We can also immediately write down the BD correction, $v_\epsilon = v_F - \frac{v''(\alpha_F)\pi^2\alpha_F^2}{(\ln\epsilon)^2}$. A graph of Snyder velocity with and without the correction is shown in Fig. 4. We see that the larger r_S is, the larger the correction according to BD is, since as discussed above, increasing r_S corresponds to decreasing the strength of diffusion in our model.

3. EXPONENTIALLY DISTRIBUTED HOPPING WITH A REACTION-RATE GRADIENT

In a previous work[15,16], we studied the case of fronts propagating into an unstable state up a reaction-rate gradient. We focused again on the $A + B \to 2A$ reaction [3], with an initial mean number N of A particles only in the region $x < x_0$ and B particles only, with the same mean density N, for $x > x_0$, but now with a reaction probability that depended linearly on spatial position. This type of gradient would be a natural consequence of spatial inhomogeneity, or could be imposed via a temperature gradient in a chemical reaction analog. Also, this

type of system arises naturally in models of Darwinian evolution[19,21], (where fitness x is the independent variable; the birth-rate, akin to the reaction-rate here, is proportional to fitness). The naive equation describing such a model is the Fisher equation (1) with a reaction strength $r = r_a(x)$ varying linearly in space

$$r_a(x) = \max(r_{\min}, r_0 + \alpha x). \tag{43}$$

where $r_{\min}$ is introduced to ensure that the reaction rate stays positive far behind the front, and has no effect on the velocity. This model gives rise to an accelerating front. We also introduced a *quasi-static* version of the model, wherein the reaction rate function moves along with the front:

$$r_q(x) = \max(r_{\min}, \tilde{r}_0 + \alpha(x - x_f)), \tag{44}$$

with x_f is the instantaneous front position. This quasi-static problem should lead to a translation-invariant front with fixed speed $v_q(\tilde{r}_0, \alpha)$. Although important on its own, one might also try to view the quasi-static problem as a zeroth-order approximation to the original model, (the *absolute* gradient case), where by ignoring the acceleration, one obtains an adiabatic approximation to the velocity $v(t; r_0, \alpha) \simeq v_q(\tilde{r}_0(t), \alpha)$ with $\tilde{r}_0(t) = r_0 + \alpha x_f(t)$. In both models, fluctuations become crucial due to the reaction gradient and the presence of the gradient leads to a new class of fronts. One characteristic of this new class is the divergence of the front velocity with N. We found that, to leading order, the velocity of the front in the continuum limit diverges as $\ln^{1/3}(N)$, and to leading order on a lattice, the velocity diverges as $\sqrt{\ln N}$. It should be noted that in both cases the leading order does not yield an accurate solution, and the next order correction must be taken into account.

Given that the nature of the divergence of the velocity with N depends on the microscopic implementation of diffusion (continuum versus lattice), it is natural to investigate this question for our model with exponentially distributed hopping. Here, we chose to work on a lattice (with spacing a); we will see in the end that the results here are not sensitive to the presence of the lattice. The model we study is:

$$\begin{aligned}\frac{\partial \phi_i}{\partial t} &= D\frac{(e^\gamma - 1)^3}{a^2 e^\gamma (e^\gamma + 1)}\left[\sum_{j=1}^{\infty}(e^{-\gamma j}(\phi_{i+j} + \phi_{i-j})) - 2\frac{\phi_i}{e^\gamma - 1}\right] \\ &\quad + r(i)\phi_i(1 - \phi_i)\theta(\phi_i - \epsilon),\end{aligned} \tag{45}$$

where $\gamma \equiv \beta a$ is the rate of exponential falloff of the hopping between successive lattice sites. It is easy to verify that this model reproduces continuum diffusion with coefficient D for sufficiently smooth fields ϕ_i. We choose to focus on the quasi-static problem, as the presence of a steady-state solution makes the problem analytically tractable. The steady-state solution on the lattice has the Slepyan[26]

form

$$\phi_i(t) = \phi(t - ia/v) \tag{46}$$

so that each lattice point experiences the same history, with a time shift. We define the continuous variable $z = -v(t - ia/v)$, in terms of which

$$0 = D\frac{(e^\gamma - 1)^3}{a^2 e^\gamma (e^\gamma + 1)}\left[\sum_{j=1}^{\infty}\left[e^{-\gamma j}(\phi(z + aj) + \phi(z - aj))\right] - 2\frac{\phi(z)}{e^\gamma - 1}\right]$$
$$+ r(z)\phi(z)(1 - \phi(z))\theta(\phi(z) - \epsilon) + v\phi'(z), \tag{47}$$

We wish to solve this equation for small ϵ, assuming that v will be large in this limit. Relying on our previous analysis of the nearest-neighbor hopping problem[15,16], we expect that the leading order solution for the velocity comes from the region of the front where ϕ is small, so the nonlinear ϕ^2 term can be dropped. We assume[15,21,27] a WKB-type solution $\phi(z) = e^{S(z)}$, and expand $S(z \pm aj) \approx S(z) \pm ajS'$, so equation (47) reduces to

$$0 = \frac{4D}{a^2}(e^\gamma - 1)^2\frac{\sinh^2(aS'/2)}{e^{2\gamma} + 1 - 2e^\gamma\cosh(S'a)} + r_0 + \alpha z + vS'. \tag{48}$$

As in the nearest-neighbor hopping problem, the only way to match to the post-cutoff solution is to require that the front be close to the classical turning point. In order to find the turning point, we need to equate the derivative of (48) with respect to S' to zero. Doing so we get:

$$0 = \frac{2D}{a}(e^\gamma - 1)^4\frac{\sinh(S'_*a)}{(e^{2\gamma} + 1 - 2e^\gamma\cosh(S'_*a))^2} + v. \tag{49}$$

where S'_* is the value of S' at the turning point. For large γ, Eq. (49) indeed matches the nearest-neighbor hopping result. For large v, the denominator of the first term in Eq. (49) has to be close to 0 in order to balance the second term. As the denominator vanishes if $aS'_* = -\gamma$, this gives

$$S'_* = -\frac{\gamma}{a} + \frac{\sqrt{\frac{D}{2a^3}e^{-2\gamma}\frac{(e^\gamma - 1)^4}{\sinh(\gamma)}}}{\sqrt{v}} \tag{50}$$

which is correct for $v \gg D\gamma/a$. From (50) one can obtain that, for fixed $\beta \equiv \gamma/a$, S'_* is only weakly dependent on a for $0 \le a \le 1$ as long as β is not too large, $\beta \le 2$. For example, for $\beta = 1$, $S'_* = -1 + \sqrt{D/v}$ for $a \to 0$ and $-1 + 1.0019\sqrt{D/v}$ for $a = 1$. This is reasonable, since the long-range nature of the hopping (for not too large β's), smooths over the lattice structure.

The fact that $|S'_*|$ is bounded by β is the unique feature of our exponentially-distributed hopping. We remind the reader that for standard continuum diffusion, $S'_* = -v/(2D)$, and so $|S'_*|$ grows unboundedly with v, while for nearest-neighbor

hopping, $|S'_*|$, though not linearly dependent, still grows logarithmically with v. The faster the growth of $|S'_*|$, the weaker the dependence of the velocity on $\ln(\epsilon)$. This confirms our initial intuition that the exponentially distributed hopping model should be more sensitive to fluctuations that even the nearest-neighbor hopping model. It also reiterates why the lattice parameter a is not important (for β not large), since the rate of exponential falloff of ϕ is bounded by β, and so never gets so large as to be affected by the lattice.

Since the turning point is close to the cutoff point, the dominant contribution to the value of ϕ is e^{S_*}, where S_* is the value of S at the turning point (assuming $S(0) = 0$). This is given as:

$$\begin{aligned} S_* &= \int_0^{z_*} dz S' = \int_0^{S'_*} dS' S' \frac{dz}{dS'} \\ &= \int_0^{S'_*} dS' S' \left(-\frac{1}{\alpha}\right) \left[\frac{2D}{a} \frac{(e^\gamma - 1)^4 \sinh(S'a)}{(e^{2\gamma} + 1 - 2e^\gamma \cosh(S'a))^2} + v\right] \\ &= -\frac{D(e^\gamma - 1)^4}{\alpha a^2 e^\gamma} \left[\frac{S'_*}{e^{2\gamma} + 1 - 2e^\gamma \cosh(S'_* a)} - \frac{1}{a(e^{2\gamma} - 1)} \ln\left(\frac{e^{\gamma + aS'_*} - 1}{e^\gamma - e^{aS'_*}}\right)\right] \\ &\quad - \frac{v(S'_*)^2}{2\alpha} \end{aligned} \tag{51}$$

To leading order, $\phi_c \equiv \phi(z_c) = e^{S_*}$. In order to get the correction for S_*, we write, in the vicinity of the turning point,

$$\phi(z) = e^{S'_* z} \psi(z). \tag{52}$$

Equation (52) smooths the variation between lattice points in the vicinity of the turning point, so we can expand $\psi(z \pm aj)$ in a Taylor series, $\psi(z \pm aj) \approx \psi(z) \pm aj\psi'(z) + (aj)^2 \psi''(z)/2$. Doing this and performing the sums over j yields, after some algebra,

$$\begin{aligned} 0 &= D \frac{(e^\gamma - 1)^4 \left[(e^{2\gamma} + 1)\cosh(S'_* a) + 2e^\gamma \cosh^2(S'_* a) - 4e^\gamma\right]}{(e^{2\gamma} + 1 - 2e^\gamma \cosh(S'_* a))^3} \psi''(z) \\ &\quad + \alpha(z - z_*)\psi(z) \end{aligned} \tag{53}$$

This is the Airy equation. The solution of (53) is

$$\psi(z) = \mathrm{Ai}\left(\frac{z_* - z}{\ell}\right). \tag{54}$$

where we have introduced the length

$$\ell = \left(\frac{D(e^\gamma - 1)^4 \left[(e^{2\gamma} + 1)\cosh(S'_* a) + 2e^\gamma \cosh^2(S'_* a) - 4e^\gamma\right]}{\alpha(e^{2\gamma} + 1 - 2e^\gamma \cosh(S'_* a))^3}\right)^{\frac{1}{3}}. \tag{55}$$

Since the first zero of the Airy function is at -2.338, this implies that the zero of ψ lies a distance of 2.338ℓ beyond the turning point. To leading order, $\ln\phi$ decreases by an amount $2.338S'_*\ell$ over this distance. Adding this to Eq. (51) yields:

$$\ln\left(\frac{1}{\epsilon}\right) = \frac{D(e^\gamma-1)^4}{\alpha a^2 e^\gamma}\left[\frac{S'_*}{e^{2\gamma}+1-2e^\gamma\cosh(S'_*a)} - \frac{1}{a(e^{2\gamma}-1)} \times \ln\left(\frac{e^{\gamma+aS'_*}-1}{e^\gamma - e^{aS'_*}}\right)\right] + \frac{1}{2\alpha}(S'_*)^2 v - 2.338S'_*\left(\frac{\alpha}{D(e^\gamma-1)^4}\right)^{-\frac{1}{3}} \times \left(\frac{(e^{2\gamma}+1-2e^\gamma\cosh(S'_*a))^3}{\left[(e^{2\gamma}+1)\cosh(S'_*a)+2e^\gamma\cosh^2(S'_*a)-4e^\gamma\right]}\right)^{-\frac{1}{3}} \tag{56}$$

Again, this solution matches our previous solution for $\beta >> 1$[15,16]. In the continuum limit, which as we noted above is accurate for $\beta \leq 2$, this equation becomes

$$\ln\left(\frac{1}{\epsilon}\right) = \frac{D\beta^4}{\alpha}\left[\frac{S'_*}{\beta^2-(S'_*)^2}\right] - \frac{D\beta^3}{2\alpha}\ln\left(\frac{\beta+S'_*}{\beta-S'_*}\right) + \frac{1}{2\alpha}(S'_*)^2 v - 2.338S'_*\left(\frac{\alpha}{D\beta^4}\right)^{-\frac{1}{3}}\left(\frac{\left[\beta^2-(S'_*)^2\right]^3}{\beta^2+3(S'_*)^2}\right)^{-\frac{1}{3}} \tag{57}$$

Substituting the continuum limit of our expression for S'_* in the above and expanding for large v yields

$$\ln\left(\frac{1}{\epsilon}\right) = \frac{\beta^2 v}{2\alpha} + \sqrt{v}\left[-\frac{\sqrt{2D\beta^5}}{\alpha} + 2.338\frac{2^{1/6}\sqrt{\beta}}{\alpha^{1/3}D^{1/6}}\right] + \frac{D\beta^3}{4\alpha}(2+\ln\left(\frac{8v}{D\beta}\right)) - 2.338\frac{2^{2/3}D^{1/3}\beta}{\alpha^{1/3}} \tag{58}$$

which is still fairly messy. To test these formulas, we present in Fig. 5 the velocity versus $\ln(1/\epsilon)$, comparing between Eqs. (56) and (51) and numerical results from direct integration of the time-dependent equation. We see that the agreement between theory and simulation is quite good, and that the correction term is not negligible for this range of $\ln(1/\epsilon)$.

The first interesting thing to note about our analytic result is that asymptotically, for small cutoff, the velocity is proportional to $\ln\ (1/\epsilon)$, with a coefficient *independent* of D. This is reminiscent of the "velocity without diffusion" we saw in the zero-gradient case in the absence of a cutoff. We can see this point clearly in Fig. 6 where we graph $v/\ln\ (1/\epsilon)$ as a function of $1/\sqrt{\ln(1/\epsilon)}$ for $D = 1$

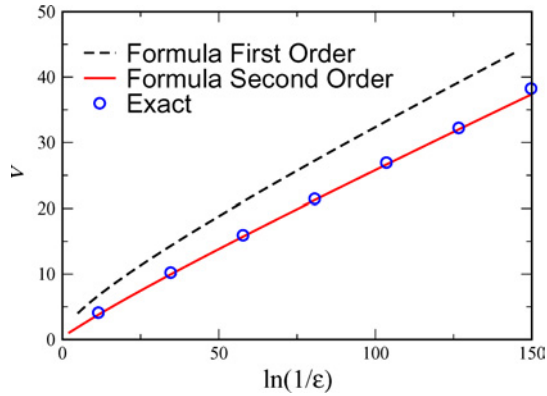

Fig. 5. v vs. $\ln(N)$ for $D = 1$, $a = 1$, $\alpha = 0.1$, $B = 1$. Numerical simulations are compared to the 1st order formula, Eq. (51) and the 2nd order formula, Eq. (56). (color online).

and $D = 4$. It is clear that the two graphs are converging to the same value of $\beta^2/(2\alpha) = 0.2$.

In Fig. 7 we present results for v versus α, again comparing the analytic formulas Eqs. (56) and (51) to the results of direct simulation. Again the agreement is very satisfying. For large α the "correction" term is dominant and the velocity grows as.

$$v \sim 0.1452 \frac{\ln^2(1/\epsilon)\alpha^{2/3} D^{1/3}}{\beta} \tag{59}$$

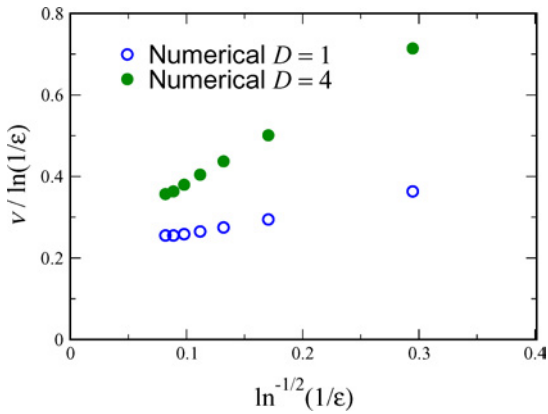

Fig. 6. $v/\ln(1/\epsilon)$ vs. $\ln^{-1/2}(1/\epsilon)$ for $D = 1$, $a = 1$, $\alpha = 0.1$, $r_0 = 1$. The data presented are from numerical simulations of the cutoff deterministic equation. (color online).

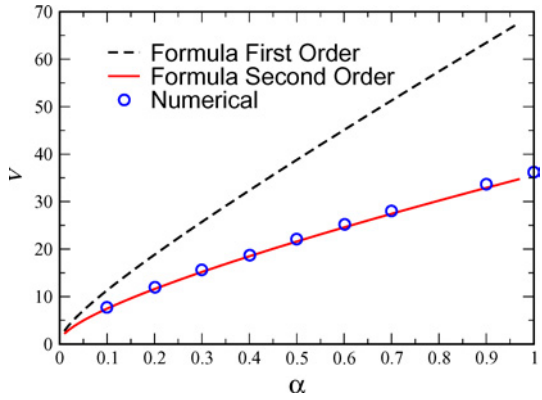

Fig. 7. v vs. α for $D = 1, \beta = 1, a = 1, r_0 = 1, \ln(N) = 25$. Numerical simulations are compared to the 1st order formula, Eq. (51) and the 2nd order formula, Eq. (56). (color online).

Unfortunately, this asymptotic result is only valid for extremely large $\alpha \gg \ln^3(1/\epsilon)$.

The dependence of the velocity on the diffusion constant D is presented in Fig. 8, where we again present a comparison with our theoretical prediction. It is seen that as D grows, v/D decreases, and so our analytic approximation for S'_* becomes increasingly less reliable. Further analysis shows that in fact for very large D, $S'_* \approx v/(2D) \ll 1$, and the calculation reverts to that of the standard continuum diffusion presented in[15], where $v \sim f(\alpha, \epsilon)D^{2/3}$, and the prefactor $f \sim (24\alpha \ln(1/\epsilon))^{1/3}$ for $\epsilon \to 0$. We can verify this result by replotting the data in Fig. 9, this time showing $v/D^{2/3}$, which is seen to be consistent with an approach to

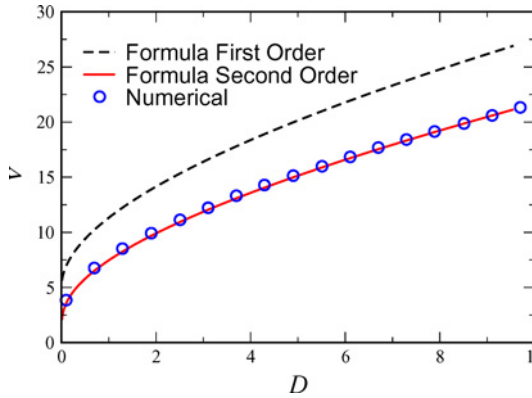

Fig. 8. v vs. D for $\beta = 1, a = 1, \alpha = 0.1, r_0 = 1, \ln(1/\epsilon) = 25$. Numerical simulations are compared to the 1st order formula, Eq. (51) and the 2nd order formula, Eq. (56). (color online).

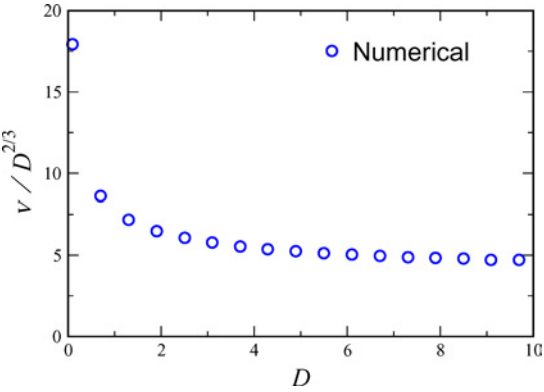

Fig. 9. $v/D^{2/3}$ vs. D for $\beta = 1$, $a = 1$, $\alpha = 0.1$, $r_0 = 1$, $\ln(1/\epsilon) = 25$. Data presented are from numerical simulations of the deterministic cutoff equation. (color online).

a constant close to $(24\alpha \ln(1/\epsilon))^{1/3} = 3.91$. This reversion to continuum diffusion for large D is reasonable, since if diffusion is fast enough, it is irrelevant how it is implemented. For extremely small D our calculation becomes unreliable, since there one is not allowed to truncate to an Airy equation. We expect, similar to what we occurs in the evolution problem, that the velocity will be proportional to D/ϵ in this limit.

Lastly, Fig. 10 shows a comparison between (56), (51) and numerical results for v vs. the rate of falloff of the hopping distribution, β. For large β, the problem reverts to the nearest neighbor hopping model, so v should approach a constant in that limit, consistent with the data presented. For small γ, again the "correction" term is dominant and we recover the large α result, Eq. (59), with v diverging as $1/\beta$. We therefore plot $v\beta$ versus β in Fig. 11, where we see that the data is consistent with $v\beta$ approaching the constant $0.1452 \ln^2(1/\epsilon)\alpha^{2/3} D^{1/3} = 19.55$ for small β.

The last task before us is to test if our cutoff theory is a good approximation for the stochastic case. The analytical procedure done above is referring to the case for which the front position x_f is defined to by $\phi(x_f) = 1/2$. For the stochastic case this procedure is ill-defined, since ϕ fluctuates. Rather, we choose to define the front by

$$x_f = \sum_k \phi_k, \tag{60}$$

Rather than redo the theory for this definition of the front, we chose the expedient of comparing the the stochastic results to numerical results that also define the front position as the sum of ϕ_k, which amounts to a shift in r_0. The comparison is shown in Fig. 12.

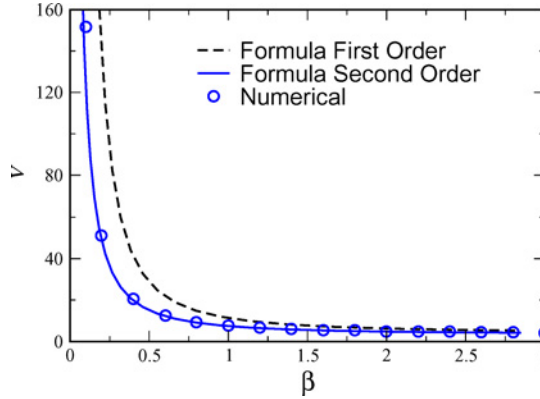

Fig. 10. v vs. β for $D = 1, a = 1, \alpha = 0.1, r_0 = 1, \ln(1/\epsilon) = 25$. Numerical simulations are compared to the 1st order formula, Eq. (51) and the 2nd order formula, Eq. (56). (color online).

As a closing remark, we note that one of the most interesting aspects of the above calculation (and the previously published calculations for the nearest neighbor hopping model) is that the result does not at all depend on form of the solution past the cutoff point; the mere existence of a cutoff is enough to force the system to the WKB turning point and hence fix the velocity.

4. SUMMARY

We have investigated herein reaction-diffusion systems in which the hopping probability exponentially decays with distance, focussing on the fluctuation

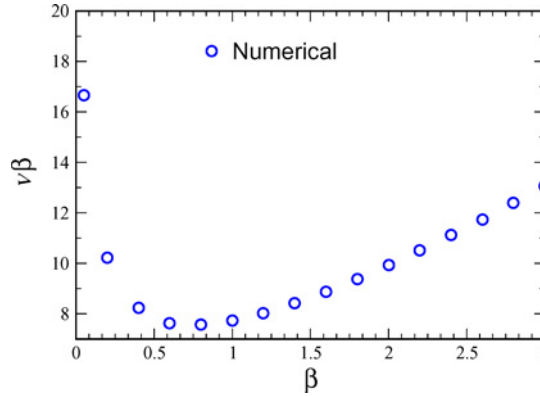

Fig. 11. $v\beta$ vs. β for $D = 1, a = 1, \alpha = 0.1, r_0 = 1, \ln(1/\epsilon) = 25$. Data presented are from numerical simulations of the deterministic cutoff equations. (color online).

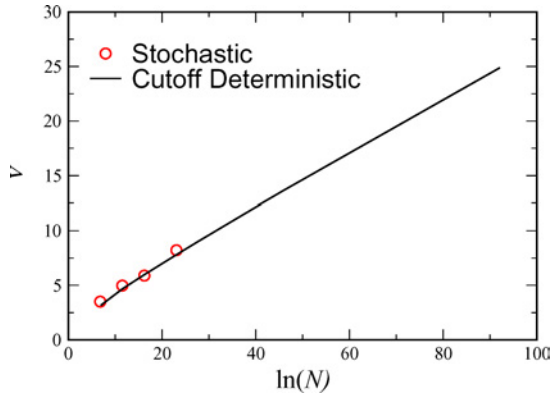

Fig. 12. Comparison between stochastic results and numerical results for v vs. $\ln(N)$ for $D = 1, a = 1$, $\alpha = 0.1, r_0 = 1$. $x_f = \sum \phi_k$. (color online).

induced anomalies seen in the same systems with continuous diffusion and nearest neighbor hopping. As in these previously studied cases, we probe the sensitivity to fluctuations by studying the dependence of the steady-state velocity on a cutoff in the reaction term when the density drops below a cutoff of the order of one particle per site. We first studied this model with no gradient, showing that, in the absence of a cutoff, the velocity does not vanish for small D. We showed that the BD correction for velocity due to the presence of a cutoff diverges in the case of small D, and calculate that the velocity actually vanishes linearly for small D in the presence of cutoff. Our model is similar to a discrete-time model describing the spread of colonies, and we show the same generic features apply to this model as well. We then studied the effect of introducing a quasi-static gradient into our model. Here, even for continuum diffusion and nearest-neighbor hoppings, fluctuation effects lead to a divergence of the velocity with increasing particle density N. We found that this phenomenon is enhanced by the exponential distributed hopping, so that the velocity diverges more strongly, as $\ln(1/\epsilon)$. In fact, for long-range hopping, $\beta \ll 1$, the velocity is proportional to $\ln^2(1/\epsilon)$. Our analytical work was confirmed by direct simulation of the cutoff deterministic equation, as well as by comparison to the original stochastic model.

An interesting question to consider is the generalization of these results to other implementations of diffusion. We speculate that the case of exponential falloff of the hopping probability is critical, in the sense that any faster falloff gives results similar to the finite-range hopping case. This distinction should arise as a result of the exponential decay of the steady-state solution. At a technical level, this is what gave rise to the existence of a maximal value of S'_*, the distinguishing feature of this calculation, compared to the finite-range and continuum hopping cases considered previously. Of course, anomalous diffusion, implemented via

Lévy flights, would lead to even more extreme behavior. This has already been seen in the context of the (uncutoff) Fisher equation[25].

APPENDIX: NUMERICAL SIMULATIONS

In the body of the paper, we have presented results from direct numerical simulations of both the deterministic cutoff reaction-diffusion equation and the stochastic particle model. Here we briefly present some relevant details of the simulation methods, especially in reference to treating in an efficient manner the long-range nature of the hopping.

Deterministic Equation

The simulations are essentially standard, using an Euler method time step. The only subtlety is in handling the hopping term efficiently. A naive treatment would involve calculating the transfer of density from every pair of sites, which is a prohibitively expensive $O(L^2)$ operation, where L is the spatial extent of the lattice.

To solve this difficulty, consider the density transfered to site i from all the sites to the left; i.e., $1, 2 \ldots i-1$. This transfered density, which we denote L_i is given by

$$L_i = \sum_{j=1}^{i-1} \phi_j e^{-\gamma(i-j)} \tag{A.1}$$

L_i satisfies a simple recursion relation:

$$L_i = (L_{i-1} + \phi_{i-1}) e^{-\gamma} \tag{A.2}$$

Thus, in one pass we can calculate how much density is transferred to every site from all its left neighbors. The density transferred from the right neighbors is done similarly, using

$$R_i = \sum_{j=i+1}^{L} \phi_j e^{-\gamma(j-i)} \tag{A.3}$$

and the recursion relation

$$R_i = (R_{i+1} + \phi_{i+1}) e^{-\gamma} \tag{A.4}$$

and making a leftward pass over the sites. The simulation is thus reduced to an $O(L)$ problem.

Stochastic Simulation

Our basic technique for simulating the stochastic model is to treat all the particles on a given site in "bulk" [5,15]. The number of particles that participate in any given process (birth, death and hopping) is given by a binomial distribution, and so can be determined by drawing a binomial deviate. The simulation performs in parallel first a hopping step, followed by a reaction step. In the reaction step, the number of B particles which transform into A's at site x is again a binomial deviate, drawn from $B(N_B(x), 1-(1-r(x)dt/N)^{N_A(x)})$. Replacing the distribution by its expected value, and setting $N_B(x) = N - N_A(x)$, and defining $\phi = N_A/N$ gives Eq. (1). A dt small enough so that less than 10% of the A, B's at a site hop and/or react in one time step is sufficient; smaller values do not alter the results.

Again, hopping in our model provides a challenge, since we cannot afford to draw a binomial deviate for every pair of sites. Rather, every time step we first determine the number of particles *leaving* that site due to the hopping, by drawing a single binomial deviate. We then determine how many of these move to the right, by drawing a second deviate. Of those moving to the left (right), we determine how many move to the nearest neighbor, by drawing a third deviate, and remove this number from the pool of left (right) movers. Then, if any particles remain in the pool, we determine how many move to the second nearest neighbor, removing these from the pool, continuing in this manner till the pool is exhausted. The number of deviates we need to choose is thus fixed (on average) by γ, independent of L.

ACKNOWLEDGMENTS

We acknowledge the support of the Israel Science Foundation. We thank Herbert Levine for useful discussions.

REFERENCES

1. A. I. Kolmogorov, I. Petrovsky, and N. Piscounov. *Moscow Univ. Bull. Math. A* **1**:1 (1937).
2. D. A. Kessler, J. Koplik, and H. Levine. *Adv. Phys.* **37**:255 (1988).
3. J. Mai, I. M. Sokolov, and A. Blumen. *Phys. Rev. Lett.* **77**:4462 (1996).
4. R. A. Fisher. *Annual Eugenics* **7**:355 (1937).
5. D. A. Kessler, Z. Ner, and L. M. Sander. *Phys. Rev. E* **58**:107 (1998).
6. E. Brunet and B. Derrida. *Phys. Rev. E* **56**:2597 (1997).
7. U. Ebert and W. van Saarloos. *Phys. Rev. Lett.* **80**:1650 (1998).
8. L. Pechenik and H. Levine. *Phys. Rev. E* **59**:3893 (1999).
9. E. Ben-Jacob, et al. *Physica D* **14**:348 (1985).
10. E. Brener, H. Levine, and Y. Tu. *Phys. Rev. Lett.* **66**:1978 (1991).
11. T. B. Kepler and A. S. Perelson. *PNAS* **92**:8219 (1995).
12. Progress has also been made on proving that modelling the stochastic process by adding appropriate multiplicative noise to the mean-field reaction-diffusion equation introduces qualitative changes

to the nature of the solution, in particular producing a reaction zone with compact support. See C. Mueller and R. B. Sowers. *J. Funct. Anal.* **128**:439 (1995). See also J. G. Conlon and C R. Doering, "On Travelling Waves for the Stochastic Fisher-Kolmogorov-Petrovsky-Piscunov Equation", (preprint) who obtain bounds on the front velocity.
13. D. A. Kessler and H. Levine., *Nature* **394**:556 (1998).
14. E. Moro, *Phys. Rev. Lett.* **87**:238303 (2001).
15. E. Cohen, D. A. Kessler, and H. Levine., *Phys. Rev. Lett.* **94**:158302 (2005).
16. E. Cohen, D. A. Kessler, and H. Levine., in preparation.
17. Experimental propagation *against* a gradient appears in D. Giller, et al., *Phys. Rev. B* **63**:220502(R) (2001).
18. M. Freidlin, in P. L. Hennequin, ed., *Lecture Notes in Mathematics* **1**527 (Springer-Verlag, Berlin, 1992).
19. L. S. Tsimring, H. Levine and D. A. Kessler., *Phys. Rev. Lett.* **76**:4440 (1996).
20. D. A. Kessler, D. Ridgway, H. Levine, and L. Tsimring., *J. Stat. Phys.* **87**:519 (1997).
21. I. M. Rouzine, J. Wakeley, and J. M. Coffin., *PNAS* **100**:587 (2003).
22. E. Cohen, D. A. Kessler and H. Levine., *Phys. Rev. Lett.* **94**: 098102 (2005).
23. R. E. Snyder., *Ecology* **84**:1333 (2003).
24. P. J. Gerrish and R. E. Lenski., *Genetica* **102/103**:127 (1998).
25. For a study of Fisher dynamics with Lévy flight transport, without a consideration of cut-off/stochastic effects, see D. del-Castillo-Negrete, B. A. Carreras, and V. E. Lynch., *Phys. Rev. Lett.* **91**:018302 (2003).
26. L. I. Slepyan., *Sov. Phys. Dokl.* **26**:538 (1981).
27. C. M. Bender and S. A. Orszag, *Advanced Mathematical Methods for Scientists and Engineers*, (Springer, New York, 1999), Sec. 5.5.